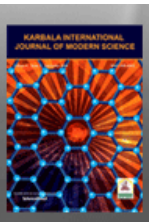

Karbala International Journal of Modern Science

Volume 7 | Issue 1 Article 8

A Non-Destructive Electromagnetic Sensing Technique to Determine Chloride Level in Maritime Concrete

Goran Omer Dr
Liverpool John Moores University, g.s.omer@2015.ljmu.ac.uk

Patryk Kot Dr
Liverpool John Moores University, p.kot@ljmu.ac.uk

William Atherton Dr
Liverpool John Moores University

Magomed Muradov Dr
Liverpool John Moores University, M.Muradov@ljmu.ac.uk

Michaela Gkantou Dr
Liverpool John Moores University, m.gkantou@ljmu.ac.uk

See next page for additional authors

A Non-Destructive Electromagnetic Sensing Technique to Determine Chloride Level in Maritime Concrete

Abstract

Deterioration of concrete due to the corrosion of reinforcement is a serious durability problem faced by the construction industry. This study aims to develop a non-destructive and real-time technique to monitor the chloride level at an early stage to prevent the development of the reinforcement's corrosion using electromagnetic spectroscopy. The experimental work was performed on 5 concrete specimens with different chloride levels at three different concrete depths (18, 40, and 70mm) using the sensor system (2-12GHz frequency range) and a chlorometer. The LM algorithm was selected to develop a prediction model for the detection of chloride ions. The results demonstrated that the proposed technique can predict the chloride level with R^2=0.986709 and RMSE =0.000120 at 5.42GHz. The results demonstrate that the sensor can predict the chloride ion content across the range of the investigated concrete depths with the percentage error of 0.034% with respect to the accuracy of the chlorometer.

Keywords

Chloride Attack; Concrete Structure; Electromagnetic Waves; Horn Antenna; Non-destructive testing.

Authors

Goran Omer Dr, Patryk Kot Dr, William Atherton Dr, Magomed Muradov Dr, Michaela Gkantou Dr, Andy Shaw Prof, Michael Riley Prof, Khalid Hashim Dr., and Ahmed Al-Shamma'a

1. Introduction

Reinforced concrete is the primary element of structures across the world because it has high compressive strength, durability and it is cost-effective [1,2]. With the beginning of the steel reinforcement bars corrosion, the losses of load-bearing capacity and the progression of stress by the development of corrosion products may result in the weakening of concrete members and subsequently the failures of the reinforced concrete structures [3,4]. Although the reinforced concrete structures are expected to be subjected to the effects of the environment, reinforced concrete structures in the marine environment are subject to very aggressive exposure conditions [5]. The deterioration of the concrete members that of the highest significance in the marine environments is the corrosions of reinforcement, which leads to cracking and spalling of the concrete covers and localized decrease in the cross-sectional of the reinforcement, and consequently, it seriously affects the load-bearing capacity of the concrete members [6,7]. The corrosion of steel within the concrete is down to two primary causes, chloride attack and carbonation. The concrete pH level reduces by the penetration of CO_2 along with the presence of moisture, leading to the formation of more general corrosion due to the de-passivation of the steel reinforcement, which is a relatively slow process depending on the porosity of the concrete cover [8−10]. Chlorides attack is categorised as the main cause of the corrosion of steel bars [11]. Therefore, the literature indicates that four factors are responsible for the corrosion of reinforcement, namely enough levels of chlorides, oxygen, moisture, and electrical conductivity.

Many concrete structures are damaged through high exposure to the seawater and spreading de-icing salt during wintertime, which leads to costly repairs and potential consequential damages to the structures [12,13]. In addition, another important factor in the marine environment is alternate wetting and drying in relation to the classification of exposure [14,15]. Currently available techniques to measure chloride levels in concrete structures are presented in Table 1. The table also provides the strengths and weaknesses of each method. The major drawback of the presented techniques is the destructive nature of the measurement; therefore, there is a need to investigate a technique for non-destructive measurement of the chloride level in real-time. In the civil engineering industry, many researchers are investigating non-destructive testing for structural health monitoring [16], namely, crack detection and voids detection [17]. In recent years, microwave technologies have been utilized across different sectors, e.g., in the food industry [18], medicine [19,20], and water industry [21−23] namely owing to the following advantages: being non-ionizing, offering high penetration, relatively low cost, providing design flexibility, non-destructive measurements, and real-time monitoring. In civil engineering, microwave technology has been investigated as an inspection tool for structural health monitoring, namely to detect structural damages (e.g. crack development in concrete beams) [1], corrosion of reinforcement bars [24,25], and monitor the excess moisture within building materials [26−28]. For example, Mamun, et al. [29] used electromagnetic induction (EMI) sensors, with two different designs, to detect the presence of the corrosive salts in the concrete bodies. The first design of the sensors was in form of single loop coils, while the second type was in form of multiple loop coils. The outcomes of their study indicated that the multiple loop coils have a better efficiency in the detection of the salts.

2. Materials and methods

2.1. Concrete specimens preparation

The concrete specimens have been built using the following mix proportions 1:1:5:0.7 Kg. The dimensions of the concrete specimens were $(1001.66 \times 43.18 \times 86.36\text{mm})$, $(120.87 \times 40.39 \times 20.19\text{mm})$, and $(40.75 \times 22.86 \times 10.16\text{mm})$ according to the internal dimensions of the waveguide (see section 2.2). Non-marine sourced sands were utilised in this work as fine aggregates. Table 2 shows the concrete composition along with the specific gravity of the used materials.

For this investigation, 5 concrete specimens were produced and submerged into water with various salt concentrations, namely 0.0%, 0.5%, 1.5%, 2.5%, and 3.5% (see Table 3) for 5 days at the ambient room temperature of ±21 °C. It is noteworthy to mention that the period of 5 days was selected according to

DOI of original article: https://doi.org/10.33640/2405-609X.2408.

https://doi.org/10.33640/2405-609X.2408

Table 1
Strengths, weaknesses, and principles of the current state of the art.

Parameter measured	NDT Method	Advantages	Limitations	Principle
Free chloride in concrete structures	Ion-Selective Electrode (ISE) [30].	It defines the stabilities of chemicals in harsh environments, it enjoys ease of fabrication via an electro–chemical reaction, it could be utilised to measure other parameters (such as temperatures, and chemicals) by adapting a suitable sensor.	The accuracy of this method is dependent on various factors such as temperature, alkalinity, and electric field presence.	The device is inserted near the rebar. Therefore, this is a partially destructive method requiring drilling into the concrete sample.
	Electrical Resistivity (ER) [31].	This method could be utilised to evaluate the chlorides concentration by measuring the coefficient of chloride diffusion.	The measurements are sensitive to the moisture content, which affects the accuracy of the results.	The device is inserted near the rebar. Therefore, this is a partially destructive method requiring drilling into the concrete sample.
	Optical Fibre Sensor [30].	It has low energy consumption. It has a high sensitivity for even low concentration of chlorides; its performance is independent of electro-magnetic fields. The sensor is better applicable to large structural applications.	Optical fiber requires a good protection level to avoid any damages during or after installation. Temperature variation can affect accuracy.	This technology includes the detection of the refractive index shifts as a result of the chloride occurrence that affects light behavior. This sensor is embedded into the structure for continuous monitoring.
Corrosion rate, percentage of corrosion, corrosion progress	Half-cell potential [32].	A simple, portable device, which produces chloride concentration contour mapping via the data logger.	Needs preparation, a saturation of the concrete surface required along with a direct electric linking to the steel bars, its accuracy is relatively low, and it requires a long testing time.	This method depends on the change in the electrical potentials because of the changes in the steel bars; these potentials are measured using a half-cell.
Determine of chloride, Partial destructive	Chlorometer device [31].	The Chlorometer test system offers a fast and accurate determination of the total chloride content in concrete. An only a small area of the concrete can be tested	Need preparation, during the test, time-consuming, high cost of extraction chloride liquid	The device is a partially destructive method requiring drilling into the concrete sample.

experimental observations; where it was noticed that 5 days were enough for moisture to penetrate the whole cross-sectional area of the samples being tested. The conductivity readings were taken from each water container with a Hanna Instruments HI933000 conductivity meter at different locations to ensure that the NaCl was dissolved.

2.2. *Electromagnetic propagation*

Electromagnetic (EM) waves are altered in various ways while they are propagating through a medium, namely, the wave can be refracted, dispersed, absorbed, or reflected. In addition, there is an irredeemable loss of energy when the waves reach an obstacle/medium, and analysis of the refracted or reflected energy can provide valuable information about the characteristics of the medium. The recorded and analyzed dielectric parameters are permittivity (ε), permeability (μ), and loss tangent (σ) of the EM wave. The values of the parameters of the dielectricity of any media are essential to determine the coefficients of transmissions and reflections. The parameters of the dielectricity

Table 2
Concrete composition.

Parameters	Mix Proportion (kg/m^3)
Ordinary Portland Cement (OPC) (CEM II 32.5R)	35.48
Fine aggregate	53.22
Coarse aggregate size (10 mm)	106.44
Water/Cement (W/C)	0.7

Table 3
Conductivity measurements with different concentrations of NaCl salt.

Saltwater concentration (%)	Conductivity readings (mS/cm)
0.0	0.176
0.5	9.4
1.5	26.6
2.5	43.1
3.5	53.2

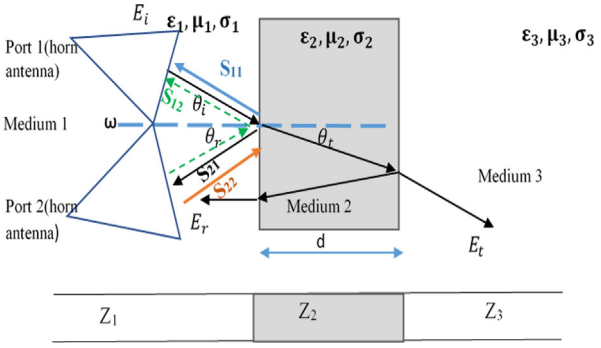

Fig. 1. Electromagnetic propagation through concrete specimen.

differ according to the composition of the material, ambient environment (such as the temperature and moisture content), and the frequency, which makes it hard to accurately calculate these parameters. However, it is very important to determine the influence of the parameters on the results [33].

Figure 1 illustrates three media, namely an air gap between the sensor system and concrete specimen, concrete specimen, and medium beyond the specimen, which encounter characteristic forms of impedance, Z_1, Z_2, and Z_3, respectively. The representation of the thickness of the concrete specimen is shown by d. As a reflection occurs, the incidence angle (θ_i), has a value that is the same for both the incident ray and the reflected ray. Furthermore, absorption causes a degree of loss whilst there is the penetration of the signal through the medium [34].

Skin depth refers to a measurement of the plane electromagnetic wave penetration into a material; the magnetic and transverse electric field decays to a value of 1/e of amplitude upon entering the material surface at that particular depth. The skin depth of EM waves is based upon the efficacy of the antenna radiation, the microwave foundation signal frequency, and the subsurface electrical characteristic. The skin depth can be calculated using permittivity and the loss tangent. The value of the losses tangents of the concrete could be explained by the following formula [35].

$$tan\delta = \frac{\epsilon_r''}{\epsilon_r'} \tag{1}$$

The concrete skin depth is calculated using Eq. (2).

$$\sigma_s = \frac{1}{\alpha}(\mathrm{m}) \tag{2}$$

where the constant of attenuation (α) can be provided by Eq. (3).

$$\alpha = \frac{\omega}{c*\sqrt{2}} * \sqrt{\epsilon_r'\mu_r'} * \sqrt{\sqrt{1+tan^2\delta}-1} \tag{3}$$

where c represents the speed of light, ϵ_r' represents relative concrete permittivity, μ_r' equates to the relative concrete permeability set to 1 for concrete and ω represents the angular frequency.

For this study, the dielectric properties were derived from S-parameter measurements (S_{21}, transmission coefficient) upon representative samples placed within the waveguides [36,37], and the use of the algorithm of Baker-Jarvis [38]. An experimental study was undertaken for determination of the imaginary and complex relative permittivity of the dry and wet samples of concrete from the measurement of S-parameters through reflection and the transmission upon three different frequency bands, namely S (2.35–2.85 GHz), C (4–7 GHz) and X (8–12 GHz) bands using WR340 (86.36 mm × 43.18 mm), WR159 (40.39 mm × 20.19 mm) and WR90 (22.86 mm × 10.16 mm) rectangular waveguides [35], respectively, along with Vector Network Analyzer (VNA) to monitor the waves (see Fig. 2). Concrete specimens were,

Figure 3 provides analyzed results for the skin depth of wet and dry concrete specimens obtained using the three waveguides. Each frequency band demonstrates different skin depth, namely the lower the frequency range, the higher the skin depth (from 15 mm to 260 mm across the full frequency range for wet and dry specimens). A skin depth threshold for the detection of chloride in reinforced concrete is 70 mm, which has been defined by XS3 of marine exposure [15]. Therefore, it was necessary to set up the sensor system to monitor this specific range for depth of concrete specimens, which led to the configuration of two horn antennas (a receiver and a transmitter) with the calculated angle in between to control the penetration of the EM signal, i.e. up to 70 mm. It must be highlighted that the change in the moisture content plays an important role in the non-destructive tests as it affects the mobility of ions and the speed of the waves.

A vector network analyzer (VNA), model Rohde & Schwarz ZNB 20 (frequency range 100 kHz to 20 GHz), was used for the measurement of the S-parameters [29,30,33] and the obtained results are presented in Fig. 4.

2.3. Experimental setup

The electromagnetic (EM) sensor was constructed using two wideband horn antennas 2–18 GHz

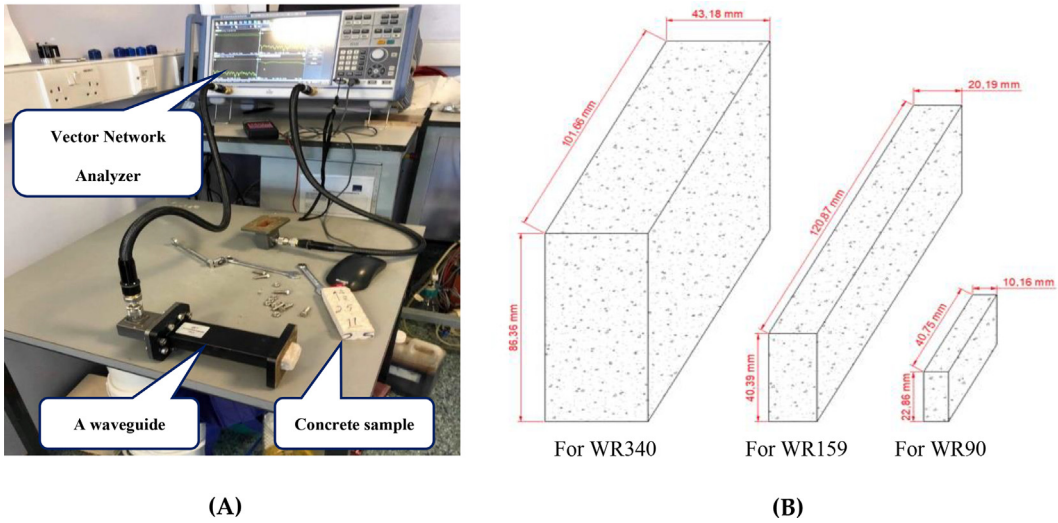

Fig. 2. A) Experimental setup for dielectric measurements, and B) Dimensions of concrete samples.

frequency (catalog number: QWH-SL-2-18-S-SG-R & Q-Par reference: QMS-00001) in this study. The sensor configuration uses the first horn antenna to act as a transmitter where the electromagnetic wave will be transmitted into the concrete specimen. The second horn antenna receives the reflected signals from the concrete being tested will be collected and used for data analysis. Figure 5 shows the sensor schematic and the sensor system.

The experimental work was carried out in the laboratory environment. The EM sensor system was connected to VNA Rohde &Schwarz ZVL13 that was connected to PC for data acquisition using a bespoke LabVIEW program. The measurements were conducted using S-parameter (S_{21}) in a frequency range of 2−12 GHz. The sensor was positioned 2 cm from the concrete specimen to perform non-destructive measurements, which were replicated 10 times for each

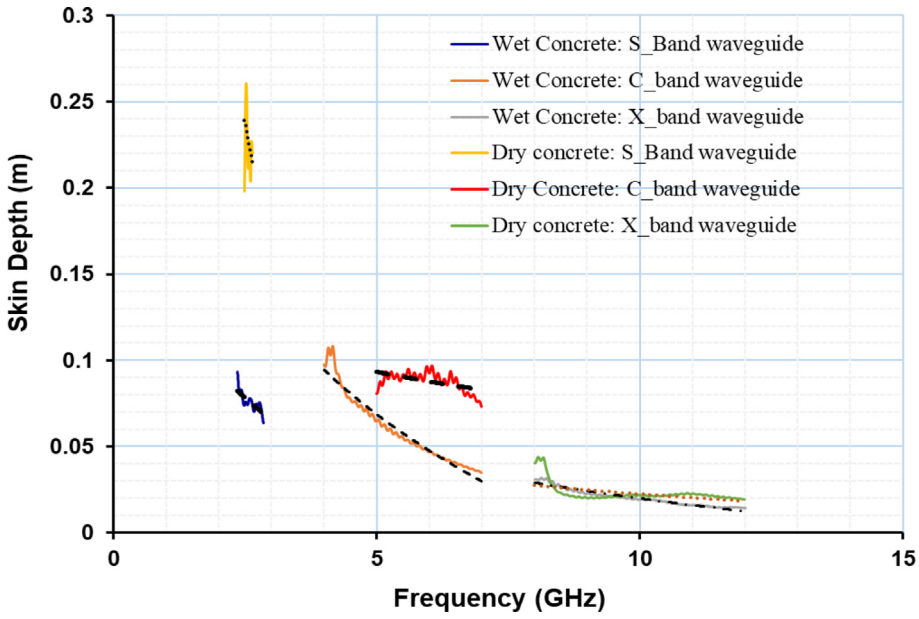

Fig. 3. Presented the skin depth of wet and dry concrete data from S-band waveguide, C-band waveguide and X-band waveguide measurements.

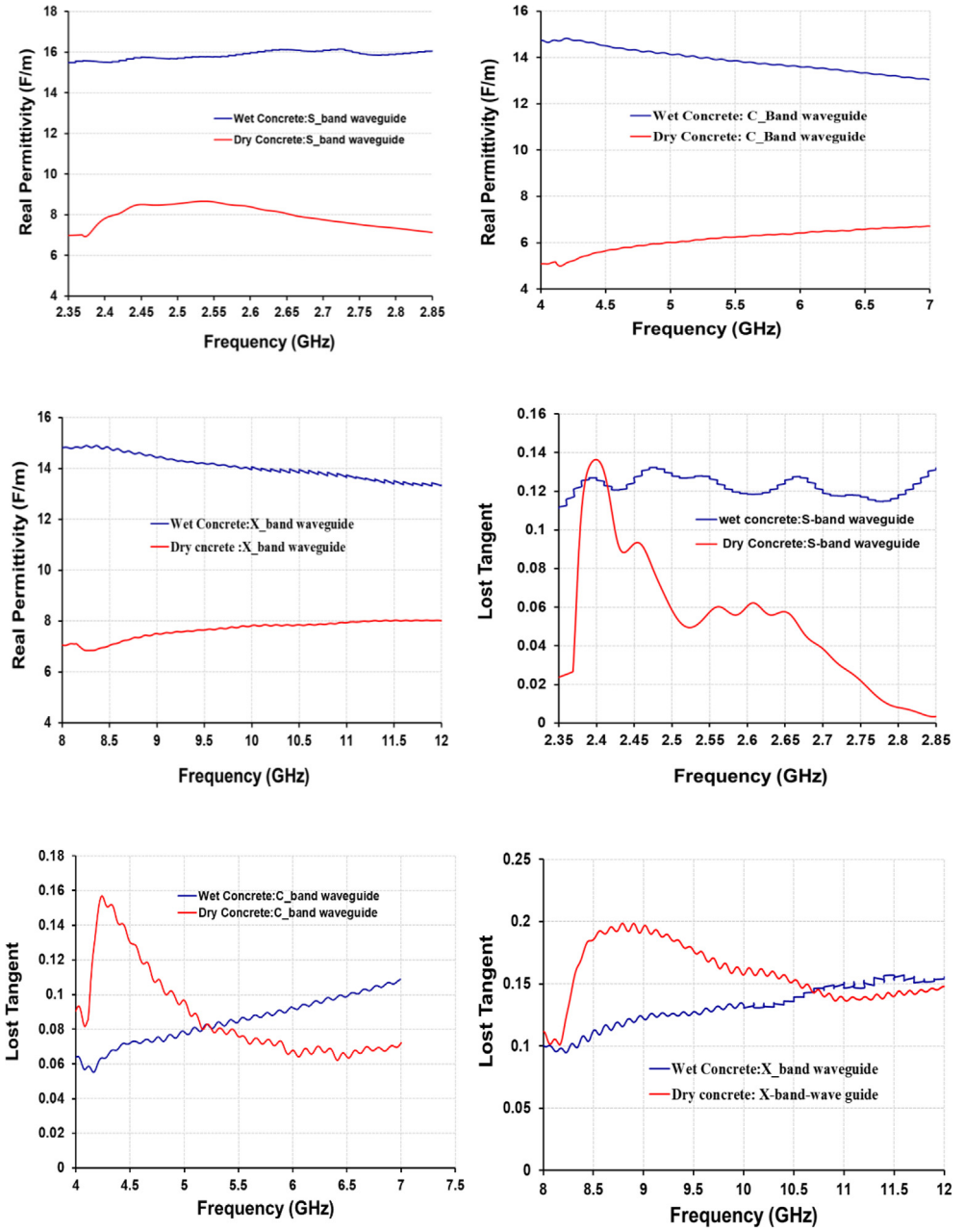

Fig. 4. Experimental results for permittivity and loss tangent measurements for wet and dry concrete.

tested specimen (see subsection 2.1). The experimental setup is shown in Fig. 6a. The chlorometer (model number C-CL-3000) was used to measure the chloride level of each specimen at three different depths, namely 18, 40, and 70 mm, which are selected according to XS3 of marine exposure. The experimental setup for the gold-standard technique is shown in Fig. 6b.

3. Results and discussions

Figure 7 presents average data of S_{21} measurements for each specimen (0.0%, 0.5%, 1.5%, 2.5%, and 3.5%), which shows obvious changes in the amplitude of the EM signal. These changes were caused by the different salt concentrations of each specimen as it is the only changed parameter in the setup. The higher

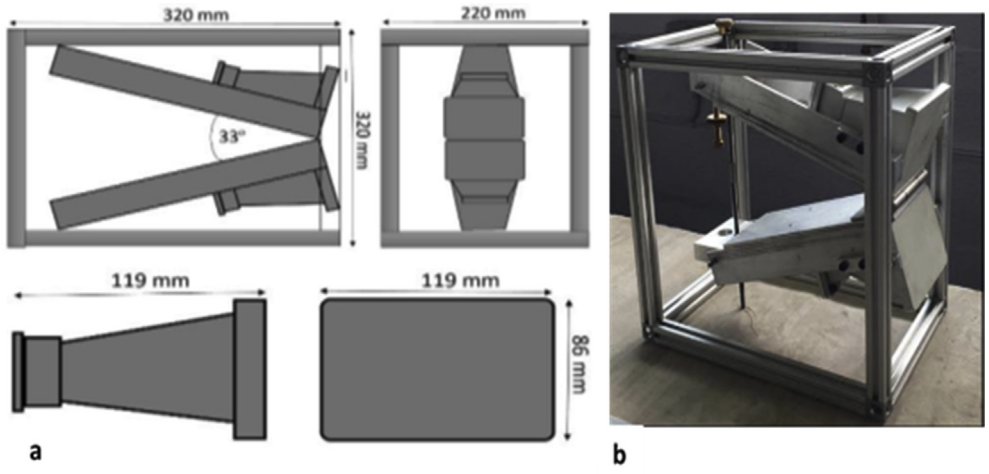

Fig. 5. a) Sensor Schematic, b) Sensor Prototype.

the salt concentration, the higher the conductivity of the specimen, which in turn alters the EM signal.

The obtained EM data were analyzed using a two-step feature selection process to identify the optimum frequency for the detection of chloride levels in the concrete specimens. The first step of analysis used an Info Gain Attribute Eval and Ranker Search method from the Weka workbench to reduce the dimensionality of the raw data based on the five different classes (salt concentrations). The second step used 10 machine learning algorithms listed in Table 4 to select the algorithm with the highest detection rate. The best results were obtained with decision tree classifier, the algorithm J48 (version C4.5) developed by Yadav et al. [39] with the detection percentage of 86% and RMSE 0.23% at 5.42 GHz. The raw S_{21} measurement at 5.42 GHz is shown in Fig. 8.

Figure 9 represents the chloride penetration at various depths with various levels of exposure using the chlorometer. While the concrete cover increases, the penetration of chloride at different concentrations decreases. This is because of the viscosity of the salt-water concentration; the permeability of the concrete and it is being well compacted during the casting. Moreover, while the water evaporated through the surface of the concrete, the salt remained inside the concrete, created a crystal and it blocked the capillary absorption to let more penetration of the solution deeper and start corrosion. The percentage of chloride per weight of cement was calculated using Eq. (4).

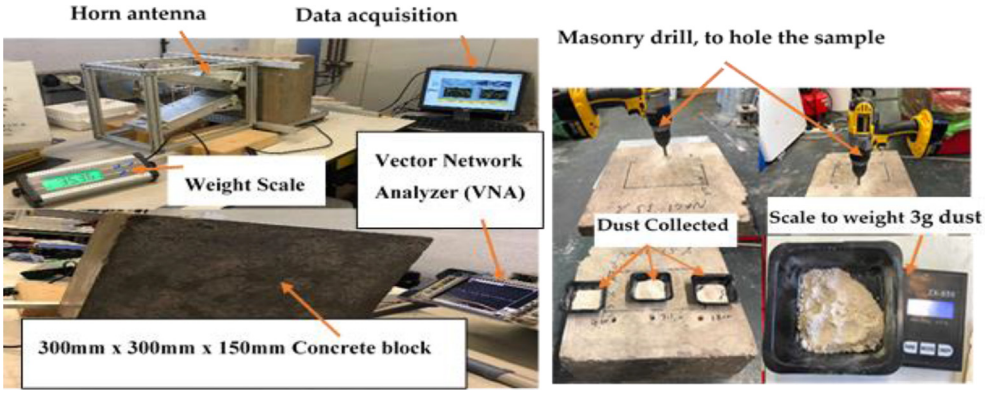

Fig. 6. Experimental setup of a) microwave sensor and b) chlorometer.

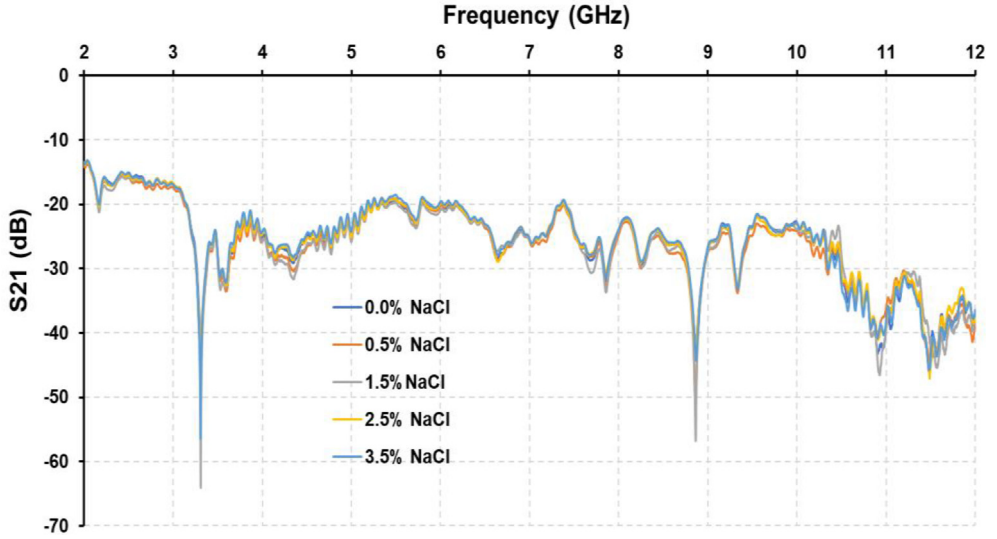

Fig. 7. Readings from the microwave horn antenna at frequency range of 2−12 GHz.

$$CL_{\text{Per WCement}}(\%) = \frac{\text{Weight of cement per sample} \times \%\text{ of chloride per weight 3 gram}}{\text{3 grams of dust per hole}} \quad (4)$$

The Artificial Neural Network (ANN) was used to develop the prediction model for chloride ions based on the chlorometer measurements at various depths (Output parameters) and sensor response at the selected 5.42 GHz frequency (Input parameter). The ANN utilized the Levenberg−Marquardt (LM) algorithm using Matlab R2019a Software [40]. The experimental dataset was classified into three sub-sets, which are 15% testing, 15% validation, and 70% training. The chloride data was formatted into 5 × 3 matrix data, i.e. 5 specimens with 3-depth chloride measurements each.

Both testing and validation datasets were plotted (calibration) to compare the observed and predicted readings of chloride ions at three different depths (see Fig. 10). There is a strong linear relationship between the measured and predicted data for the test and validation models with $R^2 = 0.9991$ and $R^2 = 0.9996$, respectively.

The performance of the LM algorithm was examined using the target values versus the predicted values as shown in Table 5. According to the results, an obvious agreement has been noticed between the observed and predicted target values basing on the

Table 4
The obtained results from different classifiers using Weka workbench.

Number	Classifier	Accuracy (%)	Means Absolute Error (%)	Root Means Square Error (%)
1	MultiScheme	20	0.3	0.4
2	Bagging	20	0.32	0.4002
3	CVParameterSelection	20	0.32	0.4
4	InputMappedClassifier	20	0.32	0.4
5	OneR	20	0.32	0.5657
6	ZeroR	20	0.32	0.4
7	REPTree	20	0.32	0.4
8	RandomTree	72	0.112	0.2366
9	DecisionStump	40	0.24	0.3464
10	J48	86	0.056	0.2266

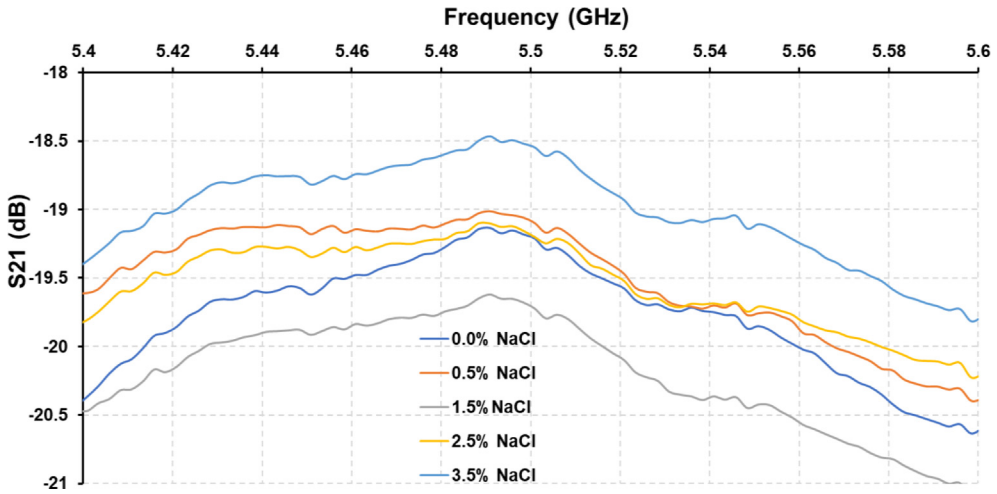

Fig. 8. Raw S21 measurements for 5 concentrations at the selected 5.42 GHz frequency.

NAE (Normalised Absolute Errors), RMSE (Root Mean Square Errors), and R^2 with the amount of chloride (%) per weight of cement at three different depths. The results have demonstrated that microwave spectroscopy could be used to measure the chloride levels in the concrete specimens at different depths at 5.42 GHz.

To verify the accuracy of the validated model developed with the ANN algorithm, the statistical chi-squared method was used to verify the data significance. Table 6 shows the final calculation of chi-squared values for the predicted percentage of chloride ion in five different salt-water concentration samples at three different depths. The results demonstrate that the electromagnetic spectroscopy can adequately predict the chloride ion content across the range of the investigated values with the percentage error of 0.034% in relation to chlorometer. It is important to mention that the EM sensors have many advantages in comparison with traditional methods, for instance, the

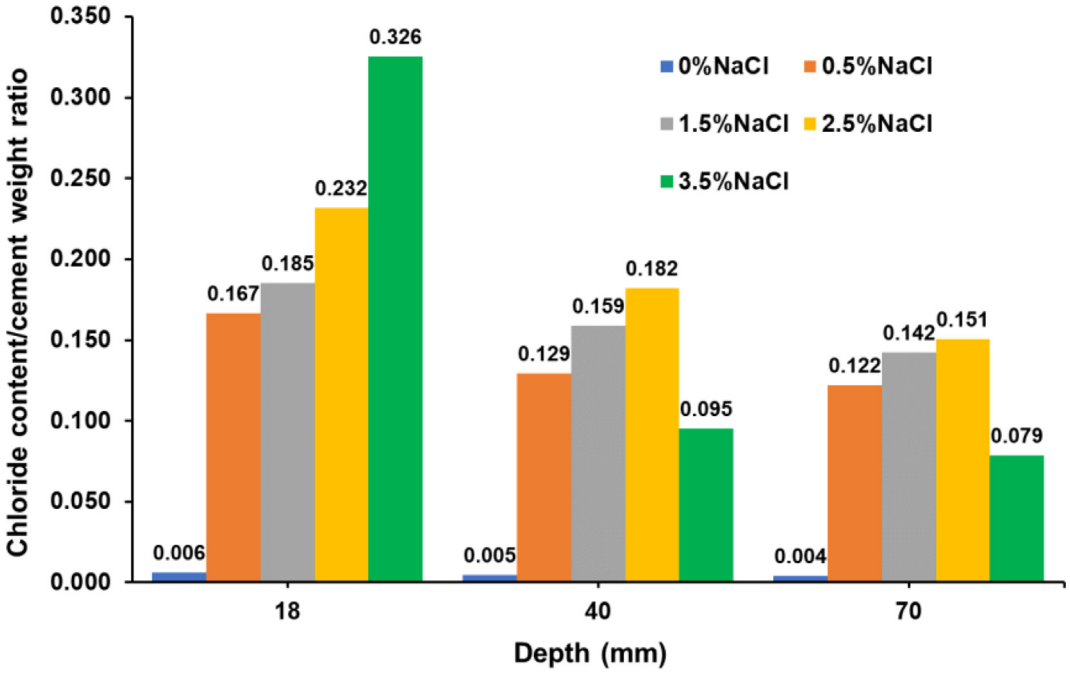

Fig. 9. Presented the % chloride per weight of cement.

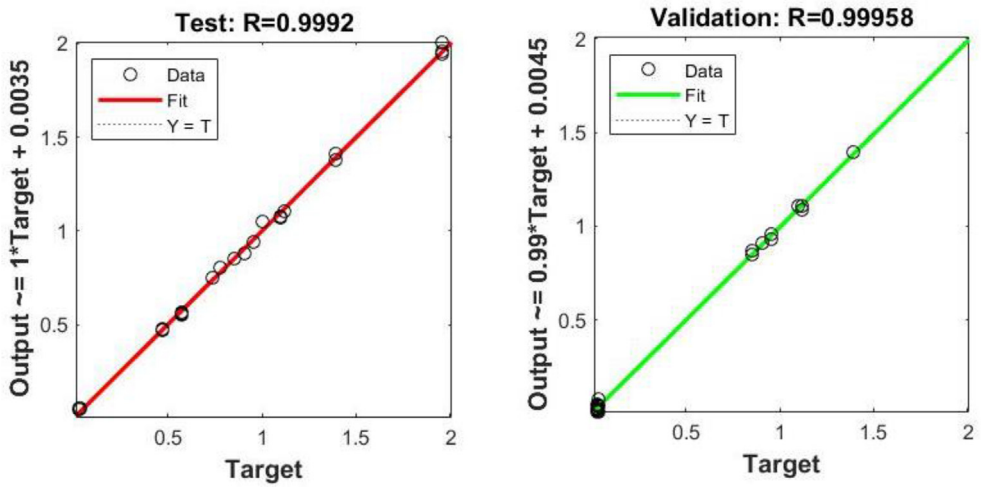

Fig. 10. Indicated the regression graphs of the experimental results against the validated chloride ions per weight of cement.

Table 5
Presented the resulting data for the observed data target and output values.

%Chloride per weight of cement	NAEs	RMSE	R^2
Depth (mm)			
18	0.000211	0.000135	0.96038
40	0.000303	0.000122	0.960397
70	0.000283	0.000106	0.960395
Total of three depth	0.000256	0.000120	0.986709

Table 6
The chi-squared values and % of error at a single frequency point (5.42 GHz).

Parameter	Chi-Squared	% of Error
Chlorometer	0.099	–
Microwave spectroscopy	0.099	0.034

EM sensors enable the operators to examine large areas at different depths, to check different chemicals, and could be operated using portable power sources, such as batteries [24,29].

4. Conclusions

This research aimed at investigating the use of electromagnetic sensors (EM) as a method for non-destructive testing of concrete specimens and to predict the chloride ions before corrosion of reinforcement can occur. Concrete specimens were produced and submerged into water with five different salt concentrations (0.0%, 0.5%, 1.5%, 2.5% and 3.5%). The obtained results demonstrated that the EM sensors could reliably be applied for detecting the chloride amount in concrete, where the best detection limit was observed at a frequency of 5.42 GHz, which were in good agreement with the readings of the chlorometer. The obtained data from both the EM sensor and chlorometer were used to develop the prediction model using ANN (LM algorithm); the dataset was classified into three sub-sets, which are 15% testing, 15% validation, and 70% training. The testing and validation models demonstrated a strong linear agreement between the experimental and predicted values with $R^2 = 0.99991$ and $R^2 = 0.99956$, respectively. In summary, the results of the present study proved the ability of the EM sensor to detect the chloride content across the investigated concrete bodies with an error margin of 0.034% with respect to the chlorometer. Further work can be conducted to test a larger number of concrete specimens to further validation and prediction model, and also by applying the EM sensors to detect the chloride content in marine structures.

Author contributions

G.O and P.K. established the ideas and methodology of this work. Following that, W.A., M.G., and M. M. performed the software, and validated and analyzed the

data. G.O, M.R, and K. H. prepared concrete block samples. G.O. and M.G. commenced data accusation. P.K., K. H., M.M, and W.A. wrote the draft of the paper. A.A., K. H., and A.S. reviewed and edited the paper. P.K. M.R. and W.A. supervised the work.

Declaration of competing interest

The authors declare no conflict of interest.

References

[1] M. Gkantou, M. Muradov, G.S. Kamaris, K. Hashim, W. Atherton, P. Kot, Novel electromagnetic sensors embedded in reinforced concrete beams for crack detection, Sensors 19 (2019) 5175−5189.

[2] A.A. Shubbar, A. Al-Shaer, R.S. AlKizwini, K. Hashim, H.A. Hawesah, M. Sadique, Investigating the influence of cement replacement by high volume of GGBS and PFA on the mechanical performance of cement mortar, J. Mater. Sci. Eng. 584 (2019) 31−38.

[3] W. Zhu, R. François, Prediction of the residual load-bearing capacity of naturally corroded beams using the variability of tension behaviour of corroded steel bars, Struct. Infrastr. Eng. 12 (2016) 143−158.

[4] A. Kadhim, M. Sadique, R. Al-Mufti, K. Hashim, Developing One-Part Alkali-Activated metakaolin/natural pozzolan Binders using Lime Waste as activation Agent, Adv. Cement Res. 32 (2020) 1−38.

[5] A.M. Ali, D. Robillard, R. Masmoudi, I.M. Khan, Experimental investigation of bond and tube thickness effect on the flexural behavior of concrete-filled FPR tube under lateral cyclic loading, J. King Saud. Univ. Eng. Sci. 31 (2019) 32−41.

[6] A. Kadhim, M. Sadique, R. Al-Mufti, K. Hashim, Long-term performance of novel high-calcium one-part alkali-activated cement developed from thermally activated lime kiln dust, J. Build. Eng. 32 (2020) 1−17.

[7] A.A. Shubbar, M. Sadique, M.S. Nasr, Z.S. Al-Khafaji, K.S. Hashim, The impact of grinding time on properties of cement mortar incorporated high volume waste paper sludge ash, Karbala Int. J. Mod. Sci. 6 (2020) 1−23.

[8] B. Díaz, L. Freire, X.R. Nóvoa, M.C. Pérez, Chloride and CO_2 transport in cement paste containing red mud, Cement Concr. Compos. 62 (2015) 178−186.

[9] H.S. Majdi, A. Shubbar, M.S. Nasr, Z.S. Al-Khafaji, H. Jafer, M. Abdulredha, Z.A. Masoodi, M. Sadique, K. Hashim, Experimental data on compressive strength and ultrasonic pulse velocity properties of sustainable mortar made with high content of GGBFS and CKD combinations, Data in Brief 31 (2020) 961−972.

[10] A.A. Shubbar, M. Sadique, H.K. Shanbara, K. Hashim, The development of a new low carbon binder for construction as an alternative to cement. In advances in sustainable construction materials and geotechnical engineering, Lecture Notes in Civil Eng. 35 (2020) 205−213.

[11] M.M. Kadhum, N.A. Alwash, W.K. Tuama, M.S. Abdulraheem, Experimental and numerical study of influence of crude oil products on the behavior of reactive powder and normal strength concrete slabs, J. King Saud Univ. Eng. Sci. 32 (2019) 293−302.

[12] A.W. Dhowian, Laboratory simulation of field preloading on Jizan sabkha soil, J. King Saud. Univ. Eng. Sci. 29 (2017) 12−21.

[13] F.P. Glasser, J. Marchand, E. Samson, Durability of concrete—degradation phenomena involving detrimental chemical reactions, Cement Concr. Res. 38 (2008) 226−246.

[14] N.N. Hilal, M.F. Sahab, T.K.M. Ali, Fresh and hardened properties of lightweight self-compacting concrete containing walnut shells as coarse aggregate, J. King Saud. Univ. Eng. Sci. 16 (2020) 1−9.

[15] W. Wu, Z. Zeng, X. Cheng, X. Li, B. Liu, Atmospheric corrosion behavior and mechanism of a Ni-advanced weathering steel in simulated tropical marine environment, J. Mater. Eng. Perform. 26 (2017) 6075−6086.

[16] C.A. Fapohunda, D.D. Daramola, Experimental study of some structural properties of concrete with fine aggregates replaced partially by pulverized termite mound (PTM), J. King Saud. Univ. Eng. Sci. 7 (2019) 1−7.

[17] A. Hussain, S. Akhtar, Review of non-destructive tests for evaluation of historic masonry and concrete structures, Arabian J. Sci. Eng. 42 (2017) 925−940.

[18] A. Mason, B. Abdullah, M. Muradov, O. Korostynska, A. Al-Shamma'a, S.G. Bjarnadottir, K. Lunde, O. Alvseik, Theoretical basis and application for measuring pork loin drip loss using microwave spectroscopy, Sensors 16 (2016) 182−195.

[19] E.C. Fear, X. Li, S.C. Hagness, M.A. Stuchly, Confocal microwave imaging for breast cancer detection: localization of tumors in three dimensions, IEEE Trans. Biomed. Eng. 49 (2002) 812−822.

[20] K.S. Hashim, A. Shaw, R. AlKhaddar, P. Kot, A. Al-Shamma'a, Water purification from metal ions in the presence of organic matter using electromagnetic radiation-assisted treatment, J. Clean Prod. 280 (2021) 1−17.

[21] S. Ryecroft, A. Shaw, P. Fergus, P. Kot, K. Hashim, A. Moody, L. Conway, A first implementation of underwater communications in raw water using the 433 MHz frequency combined with a bowtie antenna, Sensors 19 (2019) 1813−1823.

[22] S.P. Ryecroft, A. shaw, P. Fergus, P. Kot, K. Hashim, L. Conway, A novel gesomin detection method based on microwave spectroscopy, in: 12th international conference on developments in eSystems engineering (DeSE), Kazan, Russia, 2019, pp. 429−433.

[23] K.S. Hashim, S.S.M. Ali, J.K. AlRifaie, P. Kot, A. Shaw, R. Al Khaddar, Escherichia coli inactivation using a hybrid ultrasonic−electrocoagulation reactor, Chemosphere 247 (2020) 868−875.

[24] K. Mamun, F. Islam, R.N. Deo, A.A. Chand, A. Cakacaka, K.A. Prasad, An Emi Sensor for non-destructive corrosion estimation in concrete, Emi. Sensor 2 (2018) 1−14.

[25] A.A. Chand, K.A. Prasad, K. Mamun, F. Islam, Evaluation of concrete corrosion using EMI sensor, IEEE Int. Conf. Sens. Nanotechnol. (2019) 1−15.

[26] K.H. Teng, P. Kot, M. Muradov, A. Shaw, K. Hashim, M. Gkantou, A. Al-Shamma'a, Embedded smart antenna for non-destructive testing and evaluation (NDT&E) of moisture content and deterioration in concrete, Sensors 19 (2019) 547−559.

[27] P. Kot, A. Shaw, M. Riley, A. Ali, A. Cotgrave, The feasibility of using electromagnetic waves in determining membrane failure through concrete, Int. J. Civil Eng. 15 (2017) 355−362.

[28] P. Kot, A.S. Ali, A. Shaw, M. Riley, A. Alias, The application of electromagnetic waves in monitoring water infiltration on

concrete flat roof: the case of Malaysia, Const. Build Mater. 122 (2016) 435−445.

[29] K.A. Mamun, R.N. Deo, F. Islam, H.R. Pota, A.A. Chand, K.A. Prasad, A. Cakacaka, A prototype of an electromagnetic induction sensor for non-destructive estimation of the presence of corrosive chemicals ensuing concrete corrosion, Sensors 19 (2019) 1959.

[30] M. Maksimović, G.M. Stojanović, M. Radovanović, M. Malešev, V. Radonjanin, G. Radosavljević, W. Smetana, Application of a LTCC sensor for measuring moisture content of building materials, Const. Build Mater. 26 (2012) 327−333.

[31] R. Du Plooy, G. Villain, S.P. Lopes, A. Ihamouten, X. Dérobert, B. Thauvin, Electromagnetic non-destructive evaluation techniques for the monitoring of water and chloride ingress into concrete: a comparative study, Mater. Struct. 48 (2015) 369−386.

[32] J. Helal, M. Sofi, P. Mendis, Non-destructive testing of concrete: a review of methods, Elect. J. Struct. Eng. 14 (2015) 97−105.

[33] E. Richalot, M. Bonilla, M.-F. Wong, V. Fouad-Hanna, H. Baudrand, J. Wiart, Electromagnetic propagation into reinforced-concrete walls, IEEE Trans. Microw. Theor. Tech. 48 (2000) 357−366.

[34] Y. Huang, K. Boyle, Antennas: from theory to practice, John Wiley & Sons, Hoboken, 2008.

[35] S. Kim, J. Surek, J. Baker-Jarvis, Electromagnetic metrology on concrete and corrosion, J. Res. Nat. Inst. Stand. Technol. 116 (2011) 655−669.

[36] J. Baker-Jarvis, R.G. Geyer, J. Grosvenor, M.D. Janezic, C.A. Jones, B. Riddle, C.M. Weil, J. Krupka, Dielectric characterization of low-loss materials a comparison of techniques, IEEE Trans. Dielect. Electr. Insul. 5 (1998) 571−577.

[37] A. Nicolson, G. Ross, Measurement of the intrinsic properties of materials by time-domain techniques, IEEE Trans. Instru. Measure. 19 (1970) 377−382.

[38] J. Baker-Jarvis, E.J. Vanzura, W.A. Kissick, Improved technique for determining complex permittivity with the transmission/reflection method, IEEE Trans. Microw. Theor. Tech. 38 (1990) 1096−1103.

[39] A.K. Yadav, H. Malik, S. Chandel, Selection of most relevant input parameters using WEKA for artificial neural network based solar radiation prediction models, Renew Sustain. Energy Rev. 31 (2014) 509−519.

[40] B. Tarawneh, Predicting standard penetration test N-value from cone penetration test data using artificial neural networks, Geosci. Front. 8 (2017) 199−204.